ICAS 2021 SHANG HAI
International Council of the Aeronautical Sciences
32nd Congress of the International Council of the Aeronautical Sciences
September 6-10, 2021 Pudong Shangri-La, Shanghai, China

Application of vector jet control technology on aircraft longitudinal control

Liming Zheng[1], Zhiliang Bai[1], Zhou Zhou[1,2], Rui Wang[1,2]

[1]School of Aeronautics, Northwestern Polytechnical University, Xi'an 710072, China
[2]Science and Technology on UAV Laboratory, Northwestern Polytechnical University, Xi'an 710065, China

Abstract

Flow control design of airfoil can induce airflow on airfoil surface by jet flow on airfoil surface, increase energy of boundary layer, and greatly improve drag generation and stall characteristics of airfoil. Common flow control methods include trailing edge circulation control, plasma induction, combined jet (CFJ) and so on. Current studies mostly focus on improving the lift-drag characteristics of airfoils under steady or unsteady conditions by various flow control methods. In this paper, a new flow control method of vector jet is studied. On the basis of improving the lift and drag characteristics of airfoil, the effect of control moment produced by vector jet is realized. The method is applied to the horizontal tail of a specific example aircraft to realize the longitudinal control and to explore its influence law. It is compared with the conventional elevator control method. It can provide guidance for future aerodynamic design and control rate design of rudderless aircraft.

Keywords: Active Flow Control, Attitude Control, Control Allocation

1. Introduction

Active flow control technology can change the aerodynamic force and torque of the aircraft without the need of external movable rudder surface, and control the attitude of the aircraft. Jet circulation control technology is the most widely used in aircraft attitude control, which was first proposed by Davidson [1] in 1962. In the 1970s and 1990s, a large number of scholars have done a lot of basic research on jet circulation control technology [2-5]. In the 1970s, the US navy used the jet circulation control technology in the A-6A take-off and landing phase. In 1976, the University of Virginia also used the jet circulation control technology to achieve the lift, and the effect was remarkable. In 2005, Manchester University flew the tutor UAV with the jet loop control for roll control. In 2008, the team flew the DEMON [6-7] UAV with the jet loop control technology for pitch and roll control. This paper presents a new active control technology, which can have excellent control efficiency.

2. Active Flow Control

The active flow control technology adopted in this paper is different from the common technology in the past. In this paper, a group of jet nozzles arranged on the upper surface of the airfoil are used to generate the vector jet, which changes the lift characteristics of the airfoil. The nozzle P located on the upper surface of the airfoil is the main jet nozzle, which generates the jet flowing through the upper surface of the airfoil, and the nozzle located on the trailing edge of the airfoil is the control nozzle, which controls the direction of the vector jet by blowing and sucking. The lift characteristics of the airfoil are realized by the combination of two jets. The size of P is 3/1000 of the airfoil, and the size of p is 3/1000 of the airfoil. P is located at the back 20% of the airfoil.

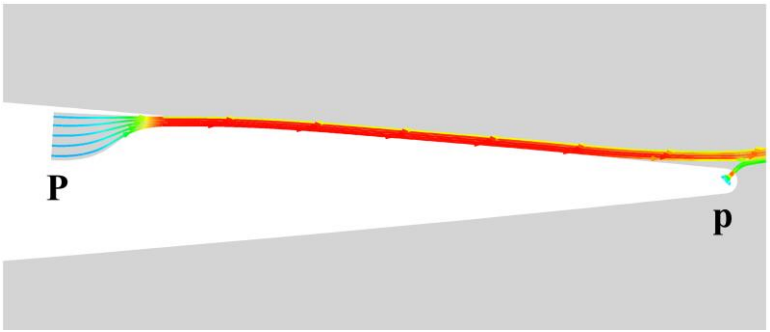

Figure 1 – Schematic diagram of nozzle, P is the upper jet nozzle, p is the vector jet nozzle.

The finite volume method is used to solve the RANS equation in CFD calculation. The integral form N-S equation used in the finite volume method is as follows:

$$\iiint_{\Omega}\left[\frac{\partial \widehat{\boldsymbol{Q}}}{\partial t}+\frac{\partial(\widehat{\boldsymbol{F}}_{\boldsymbol{i}}-\widehat{\boldsymbol{F}}_{\boldsymbol{v}})}{\partial \xi}+\frac{\partial(\widehat{\boldsymbol{G}}_{\boldsymbol{i}}-\widehat{\boldsymbol{G}}_{\boldsymbol{v}})}{\partial \eta}+\frac{\partial(\widehat{\boldsymbol{H}}_{\boldsymbol{i}}-\widehat{\boldsymbol{H}}_{\boldsymbol{v}})}{\partial \zeta}\right]d\Omega=0$$

Here, $\widehat{\boldsymbol{Q}}$ is solution vector. $\widehat{\boldsymbol{F}}_{\boldsymbol{i}},\ \widehat{\boldsymbol{G}}_{\boldsymbol{i}},\ \widehat{\boldsymbol{H}}_{\boldsymbol{i}}$ are the inviscid flux vectors in turn along the three coordinate directions. $\widehat{\boldsymbol{F}}_{\boldsymbol{v}},\ \widehat{\boldsymbol{G}}_{\boldsymbol{v}},\ \widehat{\boldsymbol{H}}_{\boldsymbol{v}}$ are the inviscid flux vectors along the three coordinate directions in turn and the space discretization of the viscous flux vector control equations along the three coordinate directions in turn. Roe-FDS format is used. Notification in Roe-FDS format is:

$$\boldsymbol{F}_{\boldsymbol{1/2}}=\frac{1}{2}(\boldsymbol{F}_{\boldsymbol{L}}+\boldsymbol{F}_{\boldsymbol{R}})-\frac{1}{2}(|\boldsymbol{F}_{\boldsymbol{R}}|-|\boldsymbol{F}_{\boldsymbol{L}}|)=\frac{1}{2}(\boldsymbol{F}_{\boldsymbol{L}}+\boldsymbol{F}_{\boldsymbol{R}})-\frac{1}{2}|\widetilde{\boldsymbol{A}}|\cdot\Delta\widetilde{\boldsymbol{Q}}$$

The non-sticking term is of second order upwind style and the sticky term is of second order central format. The turbulence model uses an equation model, Spalart-Allmaras model.

The computational grid is a non-structural grid mixed with quadrangles and triangles. The mesh quantity is 24522. The far-field range of the front and rear of the wing is 20 times the chord length of the wing. The surface boundary of the wing is the boundary of viscous matter. The nozzle is placed on the boundary of the grid and gives pressure increment to realize the jet flow. The jet flow coefficient is usually used to reflect the intensity of the jet, which is defined as:

$$c_{\mu}=\frac{\dot{m}v_{j}}{\frac{1}{2}\rho_{\infty}V_{\infty}^{2}S}$$

Here, $\dot{m}$ is the mass flow rate. v_j is the jet speed at the jet port. ρ_∞ is free inflow density. v_∞ is free inflow velocity. S is the reference area. In the paper, C_μ is the momentum coefficient of the main jet, and blowing intensity at jet control port δp is expressed as the ratio of the difference from the incoming atmospheric pressure to the incoming atmospheric pressure.

$$\delta p=\frac{p-P_{\infty}}{P_{\infty}}$$

Here, p is the increment of grid pressure at the jet control port. P_∞ is the static pressure of the incoming flow.

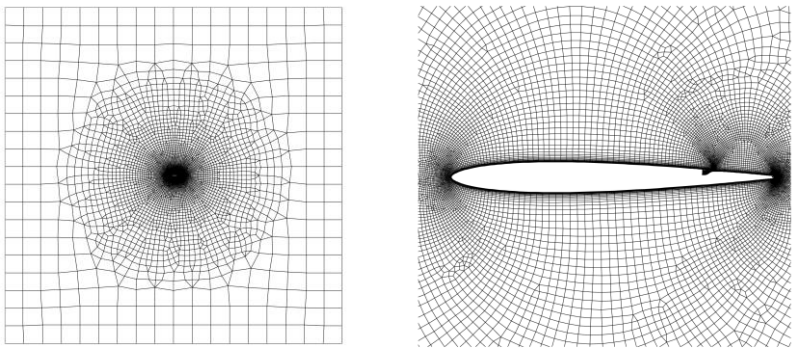

Figure 2 – Computational grid plan, Mesh around airfoil

Figure 3 show $c_\mu = 0.313$, Blowing intensity of jet control port δp from - 0.05 to 0.25:

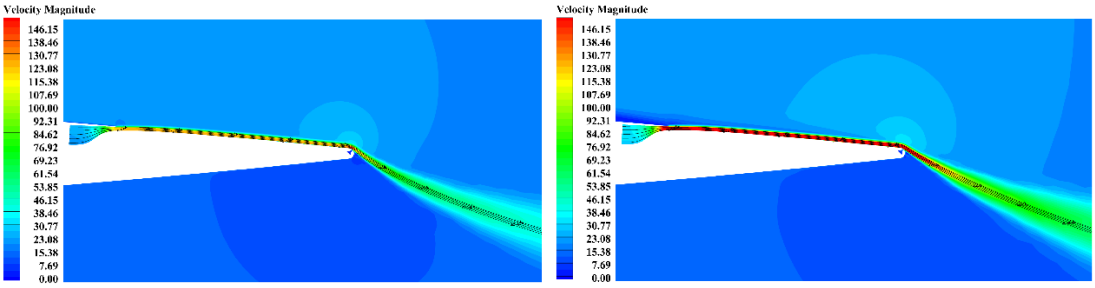

$\delta p = -0.05$ $\delta p = -0.025$

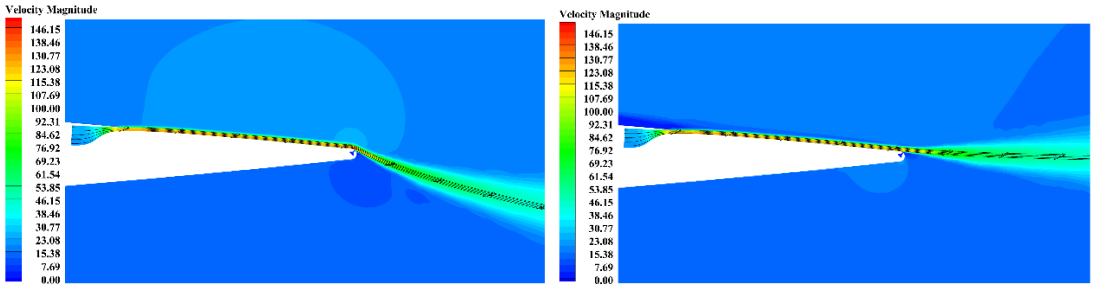

$\delta p = -0.01$ $\delta p = 0$

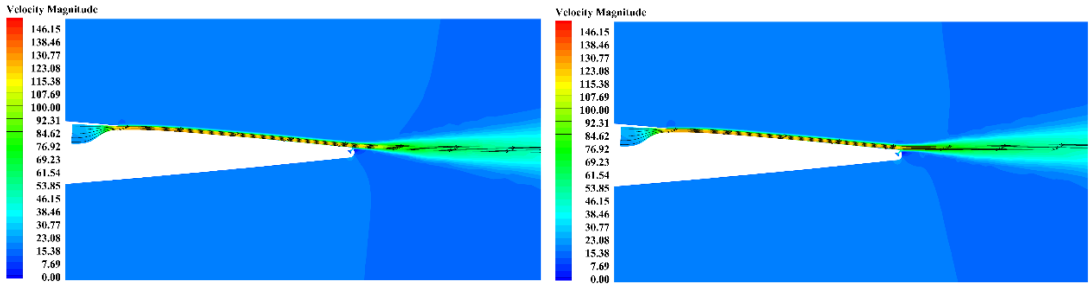

$\delta p = 0.01$ $\delta p = 0.025$

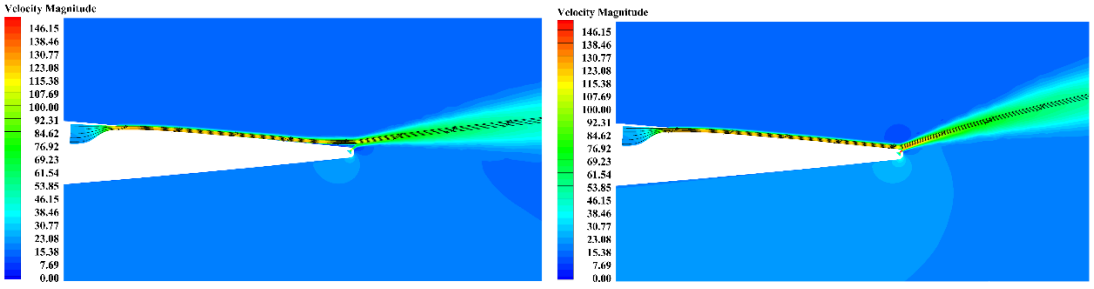

$\delta p = 0.1$ $\delta p = 0.25$

Figure 3 - Flow field diagram with different δp

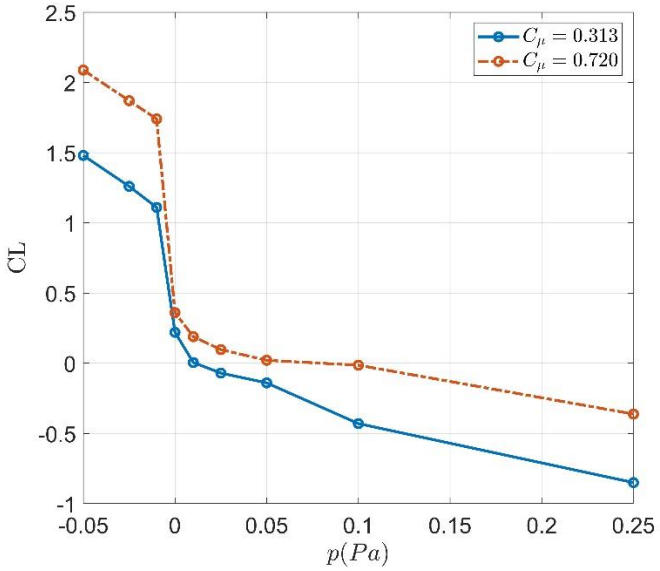

Figure 4 - The lift coefficient of the airfoil varies with C_μ and trailing edge jet pressure

3. Flight Dynamics Modeling

The aircraft used in this paper is a small aircraft with conventional layout.

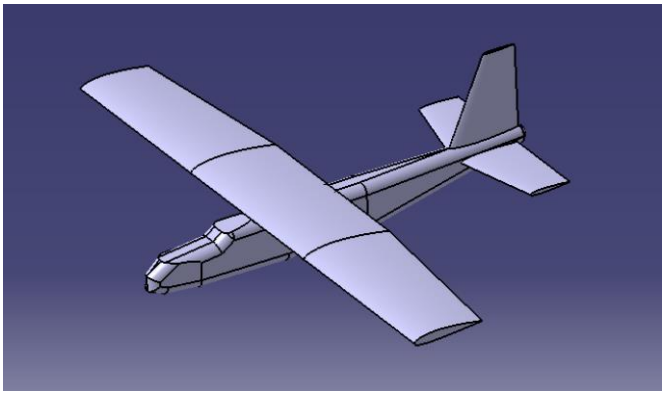

Figure 5 - The aircraft used in this paper

Table 1 - Aircraft parameters

Reference area	$0.4713m^2$
Reference chord length	0.2631m
Flat tail reference area	$0.0990m^2$
Reference wing span	1.8m
Flight weight	3kg

The vehicle uses the 6-DOF dynamic equation:

$$
\left.\begin{aligned}
&I_x\frac{dp}{dt}+(I_x-I_y)qr-I_{zx}(pq+\frac{dr}{dt})=L\\
&I_y\frac{dq}{dt}+(I_x-I_z)rp+I_{zx}(p^2-r^2)=M\\
&I_z\frac{dr}{dt}+(I_y-I_x)pq+I_{zx}(qr-\frac{dp}{dt})=N
\end{aligned}\right\}
$$

$$
\left.\begin{aligned}
&m(\frac{dV_x}{dt}+V_x\omega_y-V_y\omega_z)=F_x\\
&m(\frac{dV_y}{dt}+V_x\omega_z-V_z\omega_x)=F_y\\
&m(\frac{dV_z}{dt}+V_y\omega_x-V_x\omega_y)=F_z
\end{aligned}\right\}
$$

The required aerodynamic data are derived from CFD and Vortex Lattice Method calculation, and the mass characteristic data are derived from actual measurements.

4. Longitudinal Control

After establishing the flight dynamics simulation model in Matlab, the cruise state is first selected as the reference state, and the model is linearized by the small disturbance linearization method and is balanced at the selected cruise state points. On the basis of linearized state equation, the longitudinal control law is designed. The longitudinal control effect of vector jet control is compared with that of conventional elevator.

Table 2 - Cruise point

Cruise velocity	15m/s
Cruise angle of attack	3.5°
Cruise altitude	500m

As for the ordinary aircraft, the elevator trim angle is -0.9 degrees. Using the active flow control, the lift coefficient of horizontal tail is 0.003379.

4.1 Control Law Design

(1) Elevator control

The control law of conventional elevator adopts cascade PID, the inner loop controls the pitch angular velocity, and the outer loop controls the pitch angle.

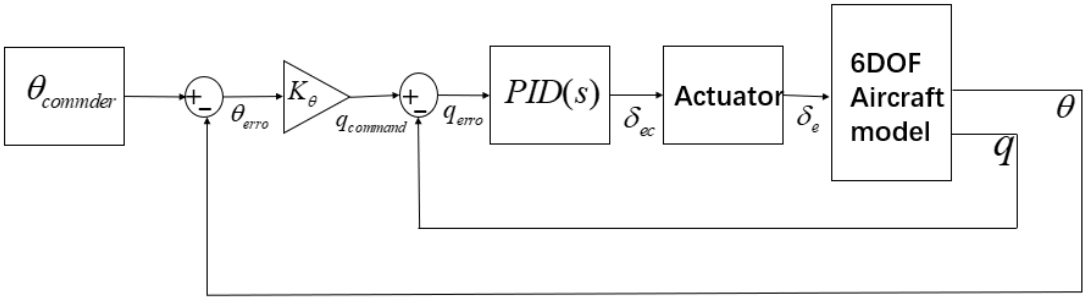

Figure 6 - Conventional elevator control

(2) Active flow control

The cascade PID is also used to control the vector jet, but there are two control variables for the trailing edge jet in this design, one is the front jet and the other is the rear blow and suction. In order to simplify the problem, cascade PID is used as a virtual control variable, which is regarded as an independent variable of two flow control variables, and two functions are used to generate two output variables by using the results of PID.

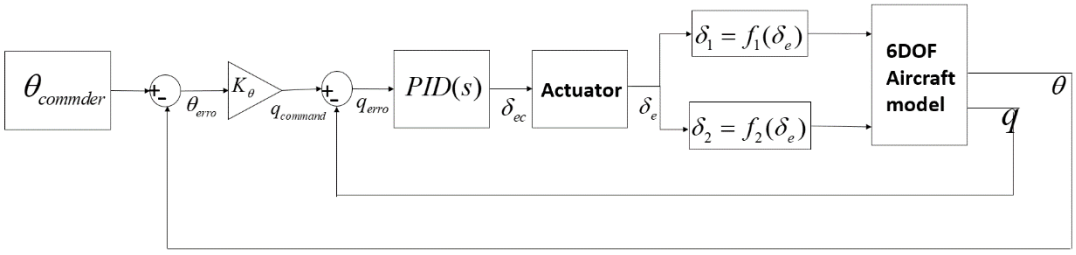

Figure 7 – Active flow control

Here, $\delta_1 = f_1(\delta_e)$ and $\delta_2 = f_2(\delta_e)$ are the functional relations between the two control variables of the given vector jet control and the virtual elevator. It is assumed that both functions are primary functions.

$$\delta_1 = C_\mu = a_1\delta_e + b_1$$
$$\delta_2 = p = a_2\delta_e + b_2$$

Table 3 – Parameters of Control Allocation

a_1	-0.5
b_1	0.4
a_2	0.1
b_2	0.001

4.2 Simulation and Results

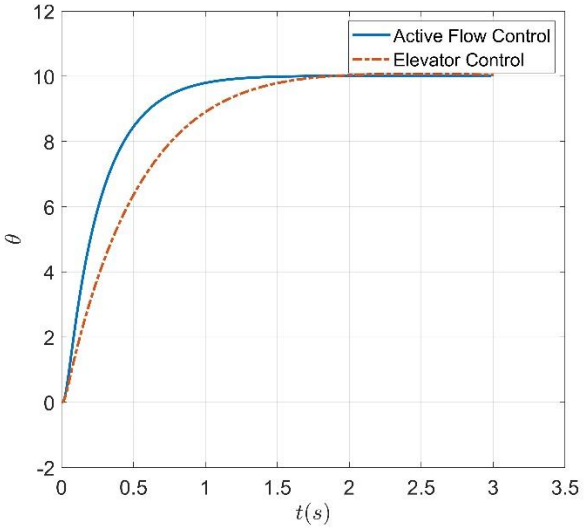

Figure 8 - Comparison of two control methods

We build a simulation model in Simulink and compare the two control methods. The results show that the active flow control method used in this paper has the same excellent effect as the elevator control, even faster, which may benefit from the stronger control efficiency of the active flow control.

5. Conclusion

This paper explores a novel active control method, and applies it to the plane tail of the aircraft. The simulation results show that it has excellent control efficiency, even better than the traditional elevator control. Although this control method has not been used in actual aircraft control, it still has great potential.

References

[1] Davidson I M. Aerofoil boundary layer control systems:US3062483A[P].1962.

[2] Englar R J. Experimental investigation of the high velocity coanda wall jet applied to bluff trailing edge circulation control airfoils[R]. DAVID W TAYLOR NAVAL SHIP RESEARCH AND DEVELOPMENT CENTER BETHESDA MD AVIATION AND SURFACE EFFECTS DEPT, 1975.

[3] Englar R J, Hemmerly R A, Moore W H, et al. Design of the circulation control wing STOL demonstrator aircraft[J]. Journal of Aircraft, 1981, 18(1): 51-58.

[4] Abramson J, Rogers E. High-speed characteristics of circulation control airfoils[C]//21st aerospace sciences meeting. 1983: 265.

[5] Holz R G, Hassan A A, Reed H L. Numerical model for circulation-control flows[J]. AIAA journal, 1994, 32(4): 701-707.

[6] Fielding J P, Lawson C P, Pires R, et al. Development of the DEMON technology demonstrator UAV[C]//27th International Congress of the Aeronautical Sciences. 2010.

[7] Yarf-Abbasi A, Fielding J. Design integration of the eclipse and demon demonstrator uavs[C]//7th AIAA ATIO Conf, 2nd CEIAT Int'l Conf on Innov and Integr in Aero Sciences, 17th LTA Systems Tech Conf; followed by 2nd TEOS Forum. 2007: 7725.